Modeling the Reversible Kinetics of Neutrophil Aggregation Under Hydrodynamic Shear

Sriram Neelamegham,* Andrew D. Taylor,# J. David Hellums,# Micah Dembo,§ C. Wayne Smith,* and Scott I. Simon*

*Section of Leukocyte Biology, Department of Pediatrics, Baylor College of Medicine; Houston, Texas 77030; #Cox Laboratories for Biomedical Engineering, Rice University, Houston, Texas 77251; and §Department of Biomedical Engineering, Boston University, Boston, Massachusetts 02215 USA

ABSTRACT Neutrophil emigration into inflamed tissue is mediated by β_2-integrin and L-selectin adhesion receptors. Homotypic neutrophil aggregation is also dependent on these molecules, and it provides a model system in which to study adhesion dynamics. In the current study we formulated a mathematical model for cellular aggregation in a linear shear field based on Smoluchowski's two-body collision theory. Neutrophil suspensions activated with chemotactic stimulus and sheared in a cone-plate viscometer rapidly aggregate. Over a range of shear rates (400–800 s^{-1}), ~90% of the single cells were recruited into aggregates ranging from doublets to groupings larger than sextuplets. The adhesion efficiency fit to these kinetics reached maximum levels of >70%. Formed aggregates remained intact and resistant to shear up to 120 s, at which time they spontaneously dissociated back to singlets. The rate of cell disaggregation was linearly proportional to the applied shear rate, and it was ~60% lower for doublets as compared to larger aggregates. By accounting for the time-dependent changes in adhesion efficiency, disaggregation rate, and the effects of aggregate geometry, we succeeded in predicting the reversible kinetics of aggregation over a wide range of shear rates and cell concentrations. The combination of viscometry with flow cytometry and mathematical analysis as presented here represents a novel approach to differentiating between the effects of hydrodynamics and the intrinsic biological processes that control cell adhesion.

INTRODUCTION

Adhesion of neutrophils to cytokine-stimulated endothelial cells under conditions of flow has been characterized as a sequential process that involves selectin and integrin adhesion receptors (Lawrence and Springer, 1991; von Andrian et al., 1991). Selectins appear to mediate cell capture and rolling by binding with rapid association (K_{on}) and dissociation (K_{off}) rate constants (Springer, 1995; Alon et al., 1995; Jones et al., 1993). This transient adhesion may allow sufficient time for the integrin molecules to engage and form stronger and more stable bonds with their ligands (Butcher, 1991; Lollo et al., 1993). In addition to heterotypic adhesion between neutrophils and the endothelium, it has also been shown that neutrophils in the flow stream can be recruited by other neutrophils that are adherent to the endothelium (Walcheck et al., 1996; Bargatze et al., 1994). The cell-surface receptors involved in homotypic neutrophil aggregation are analogous to those required for neutrophil-endothelial interactions (Taylor et al., 1996; Simon et al., 1993). The requisite receptor-ligand pairs for aggregation between neutrophils are the L-selectin receptor, which binds to an O-linked sialylated ligand (Bennett et al., 1995), and the β_2-integrin, which binds to an unidentified ligand.

Both the adhesive interactions between the neutrophil and the endothelium, and the homotypic aggregation of neutrophils, are influenced by fluid mechanical forces. An increase in shear rate leads to a reduction in the interaction time during cell collision (Taylor et al., 1996), which may, in turn, reduce the adhesion efficiency. A second consequence of an increase in shear rate is a concomitant increase in the shear and normal stresses acting between colliding cells. The resultant forces can increase both the extent of cell deformation and the tensile forces transmitted to the adhesive bonds between cells. The interplay of hydrodynamic factors and the time-dependent changes in receptor adhesivity after cell stimulation appears to determine the pattern of neutrophil adhesion over the range of shear rates found in the circulation (Finger et al., 1996; Alon et al., 1995).

In previous reports we have presented a technique that measures the kinetics of aggregation of chemotactically stimulated neutrophils subjected to shear in a magnetically stirred suspension within a test tube (Simon et al., 1990, 1992, 1993). These studies identified L-selectin and β_2-integrin as the chief receptors supporting the aggregation of neutrophils (Simon et al., 1993). The process was mathematically modeled in three discrete phases: 1) an aggregation phase, in which single neutrophils were recruited into aggregates with little disaggregation; 2) a plateau phase, in which the aggregate size distribution did not change with time; and 3) a disaggregation phase, in which formed aggregates spontaneously and rapidly broke up (Simon et al., 1990). The adhesion kinetics in the three phases were fit stepwise with empirically determined aggregation and

Received for publication 1 August 1996 and in final form 5 December 1996.

Address reprint requests to Dr. Scott I. Simon, Clinical Care Center, Suite 1130, 6621 Fannin, MC 3-2372, Houston, TX 77030-2399. Tel.: 713-770-4350; Fax: 713-770-4366; E-mail: ssimon@bcm.tmc.edu.

0006-3495/97/04/1527/14 $2.00

disaggregation rate constants. This analysis did not account for the time-dependent changes in adhesion efficiency and disaggregation kinetics, and it was limited to predicting the evolution of homotypic aggregates of up to five cells. Moreover, the previous model was applied to only a single shear rate and a limited range of cell concentrations.

In the current study, cone-plate viscometry has been used to apply a uniform and linear shear field to neutrophil suspensions stimulated with formylated chemotactic agonist (FMLP). At a given shear rate, two-body collision theory enables one to compute the cell collision frequency and the period of apparent contact between particles during collision, as well as the hydrodynamic and other interaction forces between the particles (Jeffery, 1922; Bartok and Mason, 1957; Smoluchowski, 1917). Aggregate size distribution and geometry after stimulation were determined by flow cytometry and light microscopy. These measurements were used as criteria in formulating a mathematical model for neutrophil aggregation. The model accounted for the time- and shear-dependent changes in aggregation and disaggregation kinetics. Thus we succeeded in predicting the evolution of cell aggregates over a wide range of shear rates (400–3000 s^{-1}) and cell concentrations (5×10^5 to 5×10^6 cells/ml). In this process we developed a methodology that quantitates the time-dependent changes in receptor-mediated cell adhesion.

MATERIALS AND METHODS

Reagents

Formyl-methionyl-leucyl-phenylalanine (FMLP) was purchased from Sigma Chemical Co. (St. Louis, MO). Electron microscope pure grade glutaraldehyde was obtained from Polysciences (Warrington, PA).

Experimental protocol

Fresh human blood was collected by venipuncture into a sterile syringe containing 10 units/ml of heparin. Neutrophils were isolated using a Ficoll-Hypaque density gradient (Mono-Poly resolving medium; Flow Laboratories, McLean, VA) as previously described (Simon et al., 1995) and kept at 4°C in Ca^{2+}-free HEPES buffer. Viability was measured at >95% by trypan blue exclusion. Before each experimental run, neutrophil suspensions at prescribed concentrations between 5×10^5 and 5×10^6 cells/ml were incubated for 2 min at 37°C in buffer containing 1.5 mM Ca^{2+}. The neutrophil suspension was placed on the plate of a cone-plate viscometer maintained at 37°C, and stimulated with 1 μM FMLP. Shear was initiated within 1–2 s after stimulus. Aliquots of 30 μl were taken at each sampling time for up to 10 min after stimulation and immediately fixed in 200 μl of cold 2% glutaraldehyde. A FACScan flow cytometer (Becton Dickinson Immunocytometry Systems, San Jose, CA) was used to analyze the aggregate distribution of fixed cell suspensions as described earlier (Simon et al., 1990). The neutrophil population was analyzed by gating on its characteristic forward scatter versus side scatter. Singlet neutrophils and aggregates were resolved using the autofluorescence resulting from glutaraldehyde fixation, and aggregates were quantitated as integral multiples of the singlet fluorescence channel numbers as shown in Fig. 1.

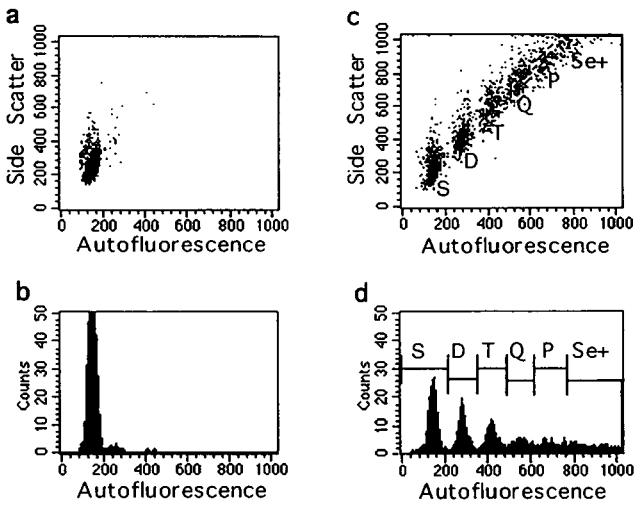

FIGURE 1 Flow cytometric detection of aggregation kinetics. Isolated neutrophils were incubated in 37°C buffer for 2 min, stimulated with 1 μM FMLP, and exposed to shear in a cone-plate viscometer. Samples were taken at various times and fixed in 2% glutaraldehyde. Two parameter dot plots of side scatter and glutaraldehyde-induced autofluorescence, along with their histogram frequency plot, used to quantify the evolution of singlets and cell aggregates, are shown. (*a*, *b*) Neutrophils before stimulation. (*c*, *d*) FMLP-stimulated cells subject to $G = 800\ s^{-1}$ for 60 s.

Cone-plate viscometry

Neutrophil suspensions were sheared in a cone-plate viscometer (Ferranti Electric, Commack, NY), which consists of a stationary plate beneath a rotating cone. The design of the viscometer makes it possible to apply a uniform shear rate to the entire sample. The shear rate, G, is independent of distance from the cone center and is given by

$$G = \frac{\omega}{\tan \theta}, \tag{1}$$

where ω is the angular velocity of the cone (radians/s), and θ is the cone angle (radians). A cone with an angle of 1° was used, and the gap between the cone and plate ranged from less than 10 μm at the center to 610 μm at the outside edge. The flow field in the experiments was laminar, and under these conditions the shear stress, τ, for a Newtonian fluid is proportional to the applied shear rate: $\tau = \mu G$. The fluid viscosity (μ) was ~0.7 cP for buffer at 37°C.

Quantifying aggregation kinetics

The particle distribution of neutrophil aggregates was determined using the histograms of fluorescence intensity Fig. 1, and as described previously (Simon et al., 1990). The extent of homotypic aggregation (% Aggregation) was expressed as the fraction of singlets recruited into larger aggregates:

$$\%\ \text{Aggregation} = \left(1 - \frac{S}{S + 2D + 3T + 4Q + 5P + 6Sx^{+}}\right) \times 100, \tag{2}$$

where the neutrophil aggregate sizes are given by S (singlets), D (doublets), T (triplets), Q (quadruplets), P (pentuplets), and Sx^+ (sextuplets and larger aggregates that could not be resolved by flow cytometric analysis). Aggregates larger than pentuplets (Sx^+) typically accounted for less than 20% of the total particles. However, under optimal shear (~800 s^{-1}) and high

cell concentration (5×10^6 cells/ml), up to 40% of the aggregates consisted of six or more cells.

Statistics

Data were analyzed using parametric paired ANOVA. Post tests were performed using the Student-Newman-Keuls test, and $p < 0.05$ was considered significant.

MATHEMATICAL MODEL FOR NEUTROPHIL AGGREGATION

Approximately 5% of the unstimulated neutrophils mixed in a cone-plate viscometer are incorporated into aggregates. However, on stimulation with FMLP (formyl-Met-Leu-Phe) and application of shear, neutrophil aggregation is a rapid and reversible process (Simon et al., 1992). Aggregates form most rapidly over the first 30 s after stimulation. After a plateau phase lasting ~2 min, the aggregates dissociate. We mathematically modeled the process to quantitate the absolute rate and extent of neutrophil aggregation and disaggregation over a range of shear rates and aggregate sizes. The model is based on a theory that describes the interaction of spherical particles mixed in a linear shear field, as formulated by Smoluchowski (Simon et al., 1990; Chandrasekhar, 1943; Smoluchowski, 1917).

The concentration C_i of aggregates of size i at any time t can be found by solving the following differential equation:

$$\frac{dC_i}{dt} = \frac{1}{2}\sum_{j=1}^{i-1} k_{i-j,j}C_{i-j}C_j - \sum_{j=1}^{N-i} k_{i,j}C_iC_j - \frac{1}{2}\sum_{j=1}^{i-1} b_{j,i}C_i + \sum_{j=i+1}^{N} b_{i,j}C_j \qquad \begin{matrix} i = 1, 2, 3 \ldots N \\ j = 2, 3 \ldots N, \end{matrix} \tag{3}$$

where $k_{i,j}$ (cells^{-1} s^{-1} cm^3) is the aggregation rate coefficient that describes the adhesion kinetics when two particles with i and j cells adhere. $b_{i,j}$ (s^{-1}) is the disaggregation rate coefficient for the dissociation of an aggregate of size j into particles of size i and $(j - i)$. N is the maximum aggregate size used in the simulation and determines the number of simultaneous differential equations solved at each time point. Experimental observations revealed that at the highest cell concentration employed and under optimum shear conditions, as many as ~40% of the aggregates contained six or more cells (Sx^+). However, under most conditions, less than 20% of the aggregates were found to be sextuplets or larger. For continuity, aggregates up to size 15 ($N = 15$) were modeled, and the aggregation kinetics of singlets through sextuplets$^+$ were fit to the experimental data. The first and second terms on the right-hand side of Eq. 3 quantify the aggregation process. The first term accounts for the rate of formation of large aggregates from two smaller aggregates (e.g., a triplet is formed from the adhesion of a singlet and a doublet). The second term accounts for particle depletion during aggregate formation (e.g., singlet and doublet populations are depleted during triplet formation). The last two terms describe the rate of disaggregation of large aggregates. The third term quantifies the rate at which aggregates break up (e.g., the rate at which a triplet breaks up into a singlet and a doublet). The fourth term accounts for the rate of formation of particles as a result of disaggregation (e.g., a singlet and a doublet are formed when a triplet disaggregates). The factor of ½ in the first and third terms is placed to avoid counting the contribution of these terms twice. The overall mass balance of the system was conserved and checked at each iteration. While modeling the entire time course of neutrophil aggregation after FMLP stimulation, we start with a population of single cells at an initial cell concentration C_o. Therefore, the initial conditions for solving Eq. 3 are

$$C_i = \begin{cases} C_0 & \text{for } i = 1 \\ 0 & \text{for } i > 1. \end{cases} \tag{4}$$

The model can also be applied for other initial conditions; for example, if the aggregate size distribution at any particular time is known and we only wish to model the aggregation kinetics beyond this point, then the initial conditions in Eq. 4 can be appropriately modified. The model is based on two key assumptions: 1) single cells and aggregates were assumed to have a spherical geometry, and 2) only single collisions between two particles were considered at any time in the iteration. The system of differential equations represented by Eq. 3 was solved simultaneously by the Runge-Kutta Fehlberg 4,5 algorithm (Shampine et al., 1976) with a variable time step on a Pentium computer.

Rate of neutrophil aggregation

Neutrophil aggregation was modeled as a two-step process:

1. Cells exposed to the linear shear field of a cone and plate viscometer collide. The uniform gradient in the velocity streamlines of a linear shear field cause the cells closer to the rotating cone surface to move faster than the cells near the stationary plate, resulting in cell-cell collisions. The intercellular collision frequency per unit volume, f_{ij}, was computed based on the physical parameters of the system: aggregate radius r_i and r_j (cm), shear rate G (s^{-1}), and concentration C_i and C_j (cells/ml) of aggregates of sizes i and j, respectively (Smoluchowski, 1917):

$$f_{ij} = \frac{2}{3}(r_i + r_j)^3 C_iC_jG. \tag{5}$$

2. Collisions between the cells result in firm adhesion with a probability that may be expressed as the adhesion efficiency (E), given by

$$E = \frac{k_{ij}C_iC_j}{f_{ij}}. \tag{6}$$

The adhesion efficiency (E) was defined as the fraction of intercellular collisions that resulted in firm adhesion, which

is always ≤ 1. Whereas $f_{i,j}$ accounts for the physical parameters of the system, efficiency is solely a function of the intrinsic properties of the cell that determine its adhesivity. These may include, but are not limited to, the number, affinity, and distribution of adhesive receptors expressed on the cell surface, their response to applied shear, and the time after stimulation.

The rate of disaggregation

The disaggregation rate is based on earlier studies that examined the kinetics of colloidal break-up (Wei et al., 1977; Pandya and Spielman, 1983). This approach has previously been applied to modeling the disaggregation of human blood platelets (Huang and Hellums, 1993). In this study, the break-up kernel $g(j)\gamma(j)p_s(j, i)$, represented the rate at which daughter fragments of size i are created by the breakup of parent particles of size j. $g(j)$ is the frequency with which aggregates of size j break up, and $\gamma(j)$ is the number of daughter fragments formed as a result of disaggregation. The resultant daughter fragment distribution is represented by the point spread function, $p_s(j, i)$. The particular expression for these functions is dependent on the nature of the disaggregation process being described. For example, disaggregation may be the result of an erosion process in which individual cells are eroded away from larger aggregates. Alternatively, it may be the result of a shattering process in which aggregates break up along points of weakness into two or more smaller aggregates. Whereas the former process forms a distribution of aggregates somewhat reduced in size and a large proportion of singlets, the latter process will result in a more random assortment of smaller aggregates. The exact nature of the disaggregation process determines the number of daughter fragments formed, $\gamma(j)$, and the point spread function, $p_s(j, i)$. The kinetics of the process determines the frequency of disaggregation, $g(j)$.

In this study we considered only the breakage of an aggregate into two fragments at any time. Hence the function describing the specific number of daughter particles, $\gamma(j)$, was lumped with the splitting frequency function, $g(j)$, and is represented by the breakup coefficient, $K_b(j)$ (s^{-1}). Mathematically, the disaggregation rate is

$$b_{ij}C_j = K_b(j)p_s(j, i)C_j. \quad (7)$$

The break-up coefficient, $K_b(j)$, is a function of the shear applied, the size of the aggregate, and the time after neutrophil activation. The point spread function $p_s(j, i)$, on the other hand, is determined by the daughter fragment distribution. Each of these functions was experimentally determined as described in Results.

RESULTS

The reversible kinetics of neutrophil aggregation after chemotactic stimulus was examined in cell suspensions sheared in a cone-plate viscometer. The distribution of aggregate sizes was measured using fluorescence flow cytometry. Aggregate geometry was determined by light microscopy. Experimentally measured parameters were used in conjunction with a mathematical model to simulate the aggregation and disaggregation kinetics of neutrophils over a range of shear rates and cell concentrations.

Kinetics of homotypic neutrophil aggregation

Neutrophil suspensions sheared in the cone-plate viscometer were fixed in glutaraldehyde at prescribed time points. The aggregate size distribution was measured by gating the histograms of glutaraldehyde autofluorescence detected on the flow cytometer (Fig. 1). The process of sample removal and fixation itself did not alter the aggregates, because the size distribution was comparable with that obtained by real-time analysis of live cells (Taylor et al., 1996; Simon et al., 1990; Rochon and Frojmovic, 1991). Freshly isolated neutrophils placed in buffer remained as singlets (~99%) before shearing and stimulation (Fig. 1, *a* and *b*). In the absence of stimulation, shear alone caused ~5% of the neutrophils to be incorporated into doublets (data not shown). On stimulation with 1 μM FMLP, the rapid onset of aggregation was observed within seconds. At 60 s poststimulation and at an optimal shear rate for aggregate formation (800 s^{-1}), >90% neutrophils were recruited into aggregates ranging from doublets to sextuplets and larger aggregates (Fig. 1, *c* and *d*).

The time course of neutrophil aggregation after chemotactic stimulus is shown in Fig. 2 for cells at a concentration of 1×10^6 cells/ml sheared at a rate of 800 s^{-1}. The distribution of singlets and aggregates was measured by gating on each particle size (singlets to sextuplets and larger aggregates) and normalizing by the total number of particles detected. The extent of aggregation (% Aggregation) was quantitated from the percentage of single neutrophils that were recruited into aggregates, as defined by Eq. 2. Three distinct phases characterized the reversible kinetics of neutrophil aggregation (Simon et al., 1990). The initial phase of rapid aggregate formation lasted from 0 to ~30 s. Single cells were rapidly taken up into aggregates, depleting the total number of singlets in the cell suspension by ~90%. Doublets are formed in the first 10 s (Fig. 2 *b*, *inset*). In the subsequent time interval (10–30 s), the doublets appear to grow in size, leading to the formation of triplets, quadruplets, and larger aggregates. Thus there was a sequential rise of aggregates of increasing size after stimulus. The rapid decrease in the particle concentration with time led to a decrease in the collision frequency and a consequent reduction in the rate of aggregation, as defined by Eqs. 5 and 6. A second factor shown to reduce the aggregation rate is the time-dependent decrease in the efficiency of cell aggregation (Rochon and Frojmovic, 1993). In the second phase of the kinetics, which lasted from ~30 to ~120 s, there was very little change in the aggregate size distribution. A rapid

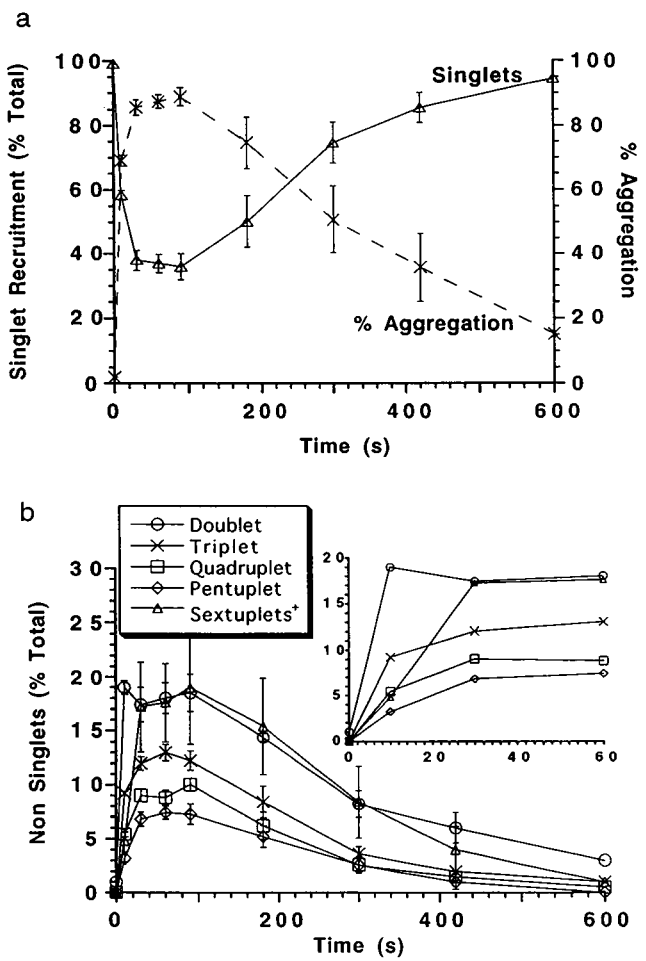

FIGURE 2 Kinetics of homotypic aggregation. Isolated neutrophils at a concentration of 1×10^6 cells/ml were stimulated with 1 μM FMLP and subject to shear at G = 800 s^{-1}. (*a*) The percentage of neutrophils recruited in aggregates (% Aggregation) and the changes in singlet concentration during the experiment. (*b*) Evolution of cell aggregates: doublets, triplets, quadruplets, pentuplets, and sextuplets$^+$. (*Inset*) Blow-up of the aggregation kinetics in the first 60 s after neutrophil stimulation. Error bars represent SEM for three experiments.

transition to disaggregation was consistently observed during the final phase, which started ~120–150 s after stimulation. The singlet population was almost totally recovered by 600 s. The three distinct phases of aggregation were consistently observed in all of the experiments, and variation among donors caused less than a 2% change in the time of onset of each of these phases. This led us to hypothesize that the kinetics of neutrophil aggregation and disaggregation are the result of changes in integrin and selectin expression and avidity over time, and the effects of shear rate and shear stress.

Cell morphology and aggregate geometry

Previous studies have shown that the increase in cell adhesiveness after stimulation with FMLP is accompanied by actin polymerization and ruffling of the neutrophil surface (Hoffstein et al., 1982; Sklar et al., 1985). We used light microscopy to examine the morphology and geometry of aggregates fixed with glutaraldehyde over the kinetics of aggregation (Fig. 3). A range of aggregate geometries was observed, from linear aggregates in which cells were at-

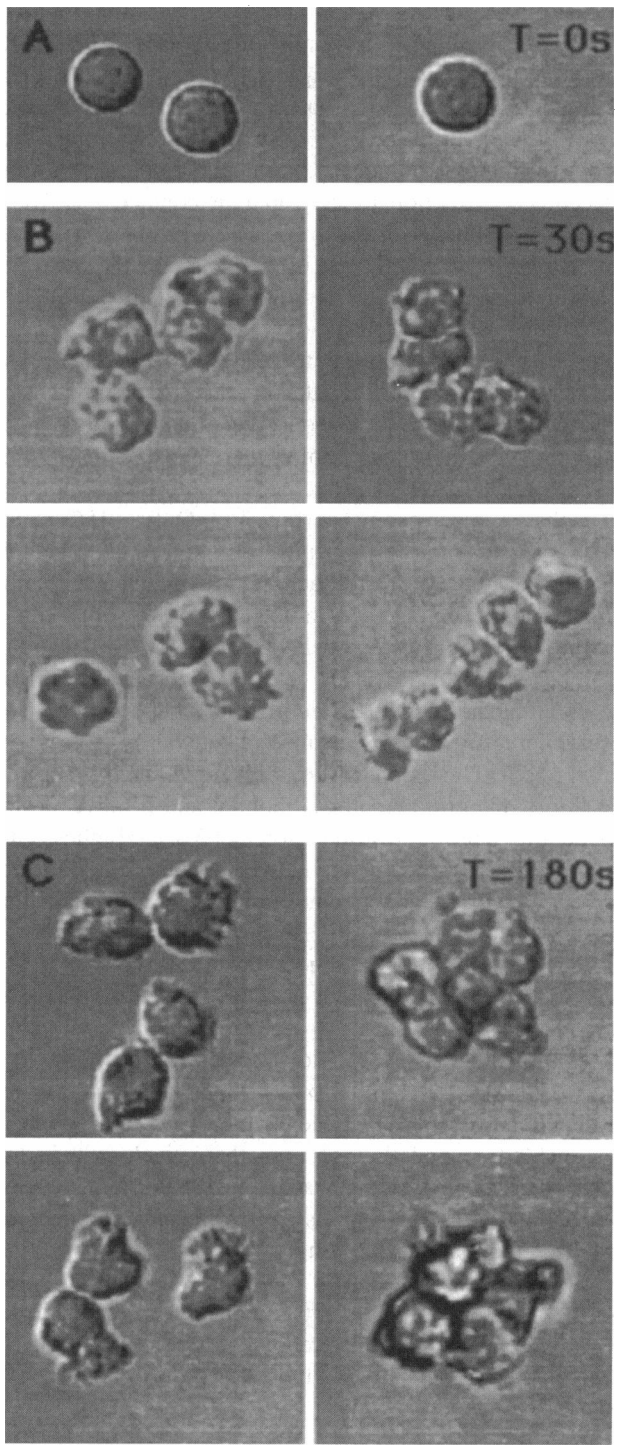

FIGURE 3 Aggregate morphology. Neutrophils stimulated with 1 μM FMLP and sheared at G = 400 s^{-1} were fixed in 2% glutaraldehyde and observed under a light microscope at various times during the experiment. (*a*) 0 s (two panels); (*b*) 30 s (four panels); (*c*) 180 s (four panels).

tached to adjacent cells at single sites of contact, to tightly packed spherical aggregates in which cells were attached to more than one cell at multiple contact sites on their surface.

Unactivated single neutrophils were smooth and rounded (Fig. 3 *a*). Within 30 s after stimulation, neutrophils adopted a ruffled appearance (Fig. 3 *b*). We have previously shown that activation is accompanied by a rapid intracellular granule fusion to the plasma membrane, which resulted in up to a 200% increase in neutrophil surface area (Simon and Schmid-Schönbein, 1988). Light microscopy revealed that the area of contact between adherent cells was greatest at 30 s (Fig. 3 *b*). In the case of doublets, we determined that ~18% of the total cell surface area was in contact with the adjacent cell (fraction of cell area in contact = 1/16 × (contact length between cells/radius of neutrophil)^2). Phase-contrast light microscopy was used to examine the geometry of aggregates composed of more than three cells. At the 30 s time point we found that ~45% of the aggregates larger than triplets were composed of linearly connected cells held together at single points of attachment (Fig. 3 *b*).

At the 180 s time point, we observed that most of the cells in aggregates larger than doublets were attached at multiple contact sites to more than one cell, resulting in a clumped rather than a linear geometry (Fig. 3 *c*). Only ~15% of the total aggregates larger than triplets were observed to be held together at single sites of attachment. Moreover, by 3 min cells adopted a bipolar morphology, with a distinct lamellipodia at the front of the cell body (Simon and Schmid-Schönbein, 1988). In a few cases we observed uropod formation at the rear of the cell. In all of the doublets we observed, the site of cell-cell attachment was away from the lamellipodia. This is consistent with previous observations that the β_2-integrin receptor is mobile, and it moves to the uropod after neutrophil stimulation by FMLP (Hughes et al., 1992). The area of contact between cells at 180 s was reduced by ~70% compared to the 30 s time point, such that doublets were attached at ~6% of the total neutrophil surface area. Apparently the contact area between cells contracted down to a smaller neck region before disaggregation (Fig. 3 *c*).

In summary, cell morphology and aggregate geometry observed under the microscope provided insight into the physical parameters that influence the aggregation process, and enabled formulation of a mathematical model. The morphological analysis indicated that in the first seconds after activation, when singlets and aggregates collided, the initial interaction was at a single site (Fig. 3 *b*). With time these aggregates appeared to minimize their surface area, and the number of sites of attachment increased. The process apparently led to the preponderance of spherical aggregates that are presumably more resistant to breakage by shear (Fig. 3 *c*).

The efficiency of neutrophil adhesion

Neutrophil surface adhesion molecules rapidly alter their expression level after activation with 1 μM FMLP. L-Selectin has been found to be shed from the neutrophil surface by ~50%, whereas Mac-1 (CD11b/CD18) was up-regulated by approximately fourfold within 2 min after stimulation (Simon et al., 1992). We have previously shown that a decrease in the expression level of L-selectin was associated with a decrease in cell adhesivity (Simon et al., 1992). In the current study we have measured the changes in adhesion efficiency over time. The strategy was to stimulate neutrophils for a defined period before applying shear in the cone-plate viscometer. Under these conditions, adhesion molecules were activated, and their affinity and expression levels changed over the lag period before shear was applied to initiate cell-cell collisions.

The kinetics of aggregate formation for neutrophils activated for 0, 30, 60, 90, or 120 s before being sheared at G = 800 s^{-1} is shown in Fig. 4 *a*. As shown, both the rate and

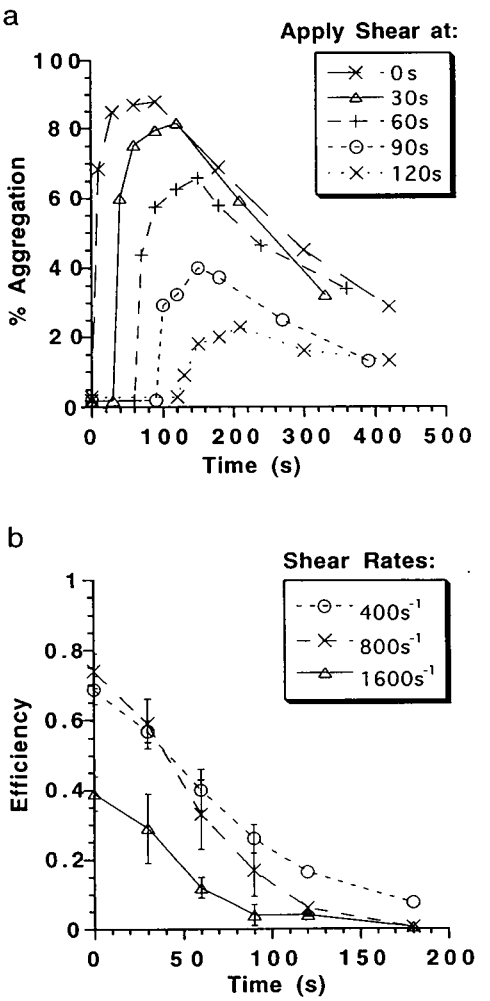

FIGURE 4 Time and shear dependence of adhesion efficiency. Neutrophils at a concentration of 1 × 10^6 cells/ml were stimulated with 1 μM FMLP for fixed time periods before application of shear. (*a*) Cells were stimulated for 0 s, 30 s, 60 s, 90 s, and 120 s before being sheared at G = 800 s^{-1}. Data represent mean for N = 3. (*b*) Adhesion efficiency with time for G = 400 s^{-1}, 800 s^{-1}, and 1600 s^{-1}. Adhesion efficiency was computed from the mathematical model over the 10 s period after shear. Error bars represent SEM for three to five experiments.

maximum extent of aggregation decreased with time after activation. In the first 10 s after the application of shear, single neutrophils were mostly recruited into doublets, with less than 10% incorporated into triplets or larger aggregates. The rate of recruitment of singlets into doublet and small aggregates over the first 10 s was mathematically fit by solving the population balance equation (Eq. 3). In these calculations, the disaggregation rate was set to zero and the frequency of collision was determined from two-body collision theory (Eq. 5). The adhesion efficiency (Eq. 6), which was assumed to be constant in the 10-s period after the application of shear, was fit to the experimental data. Fig. 4 *b* shows the time dependence of efficiency at three applied shear rates (G = 400, 800, and 1600 s^{-1}). As shown, efficiency was greatest immediately after stimulation and decreased with time. At t = 0 s, efficiency was at maximum for 400 s^{-1} and 800 s^{-1}, and ~70–75% of the collisions resulted in aggregate formation. At a shear rate of 1600 s^{-1}, efficiency was ~40%, and it further decreased to ~10% at 3000 s^{-1}. Adhesion efficiency calculated by this technique is a measure of the average rate at which single cells were recruited into doublets and small aggregates, because large aggregates were not formed in the first 10 s after application of shear.

Adhesion efficiency decreased gradually over the initial 30 s after stimulation (Fig. 4 *b*). However, after the first 30 s efficiency fell rapidly in an exponential manner to approximately zero by 180 s at all shear rates. In light of these observations, we modeled the decrease in adhesion efficiency as an exponentially decreasing process after the first 15 s as shown:

$$E = \begin{cases} E_0 & t \le 15 \text{ s} \\ E_0 e^{-\alpha(t-15)} & t > 15 \text{ s.} \end{cases} \quad (8)$$

The curve fit of efficiency over time yielded a regression coefficient of $R > 0.99$ for all shear rates. E_0 is the efficiency of cell aggregation just after stimulation. It is assumed to depend on the nature of the selectin and integrin bonds, their surface densities, and the effect of shear rate and stress on their intrinsic behavior. The adhesion exponent, α, describes the time-dependent changes in cell adhesivity. On applying and fitting the adhesion exponent over a range of shear rates, we determined the dependence of adhesion efficiency on the applied shear rate. The computed parameters (E_0 and α) are summarized in Table 1. E_0 was found to be relatively constant between shear rates of 400 s^{-1} and 800 s^{-1}, and it decreased at higher shear rates. The adhesion exponent, α, ranged from 0.013 to 0.031 (Table 1), and it increased by equal increments (~0.006) on doubling the shear rate in the range between 400 s^{-1} and 3000 s^{-1} (Table 1). Because α is small in magnitude, the exponential function can be approximated to a linearly decreasing function in the first 60 s after stimulation. Hence we concluded that the adhesivity of neutrophils stimulated with FMLP decreased linearly with time.

TABLE 1 Adhesion efficiency and disaggregation coefficient

Shear rate, G (s^{-1})	Efficiency at t = 0 s, E_0 (dimensionless)*	Adhesion exponent, α (s^{-1})*	Disaggregation coeff., K_d (s^{-1})#
400	0.68	0.013	4.8×10^{-3}
800	0.74	0.019	9.0×10^{-3}
1600	0.39	0.025	25.1×10^{-3}
3000	0.10	0.031	35.6×10^{-3}

Neutrophils at 1×10^6 cells/ml were stimulated with 1 μM FMLP and sheared in a cone-plate viscometer.

*E_0 and α were evaluated by fitting the neutrophil aggregation kinetics (Fig. 4, *a*, *b*) with the time-varying function for adhesion efficiency (Eq. 8). The disaggregation rate was set to zero.

#The disaggregation rate coefficient described in Eq. 9 was determined from the kinetics of neutrophil disaggregation (Fig. 5 *d*). The adhesion rate was set to zero.

Aggregate stability over the plateau phase

Aggregate formation decreased rapidly in the first 30 s after stimulation because of both a reduction in the total particle concentration and a simultaneous decrease in adhesion efficiency. After the initial phase of rapid aggregation, the aggregate size distribution did not change up to the ~120 s time point, at which time disaggregation ensued. The constant aggregate size distribution between 30 and 120 s may be due to two mechanisms: 1) both aggregation and disaggregation may proceed simultaneously, such that a dynamic equilibrium exists between the two processes, resulting in no net change in the size distribution; or 2) the aggregation and disaggregation rates may be close to zero, such that the aggregates formed in the first 30 s remain stably adherent over the plateau phase.

We explored the stability and strength of aggregates in the plateau and the disaggregation phases by performing two types of experiments. In the first set of experiments, we allowed aggregate formation at 1600 s^{-1} for either 30 s or 120 s before diluting the cell suspension in 20-fold excess buffer containing 1 μM FMLP and 1.5 mM Ca^{2+} (Fig. 5 *a*). This abrupt reduction in cell concentration caused the collision frequency to fall by ~400-fold (proportional to a square of the cell concentration, as shown in Eq. 5), without affecting the disaggregation kinetics. Regardless of the time of dilution, disaggregation ensued between 120 and 150 s after stimulation for both the dilution interventions and the control undiluted experiments. In all of these interventions, the aggregate size distribution remained unaltered between 30 s and 120 s. Moreover, the kinetics of disaggregation for both the dilution and the control experiments were remarkably similar. Taken together, the data support a model in which aggregates formed in the first 30 s remained stable and resistant to shear over the duration of the plateau phase.

In the second set of experiments, we assessed aggregate strength in cell suspensions stimulated and sheared at a rate of 400 s^{-1}, before a ramp increase in shear to 3000 s^{-1} at either the 30 s or the 120 s time points (Fig. 5 *b*). Stepping up the shear at 30 s did not cause aggregate break-up. Apparently, aggregates formed over the first 30 s were

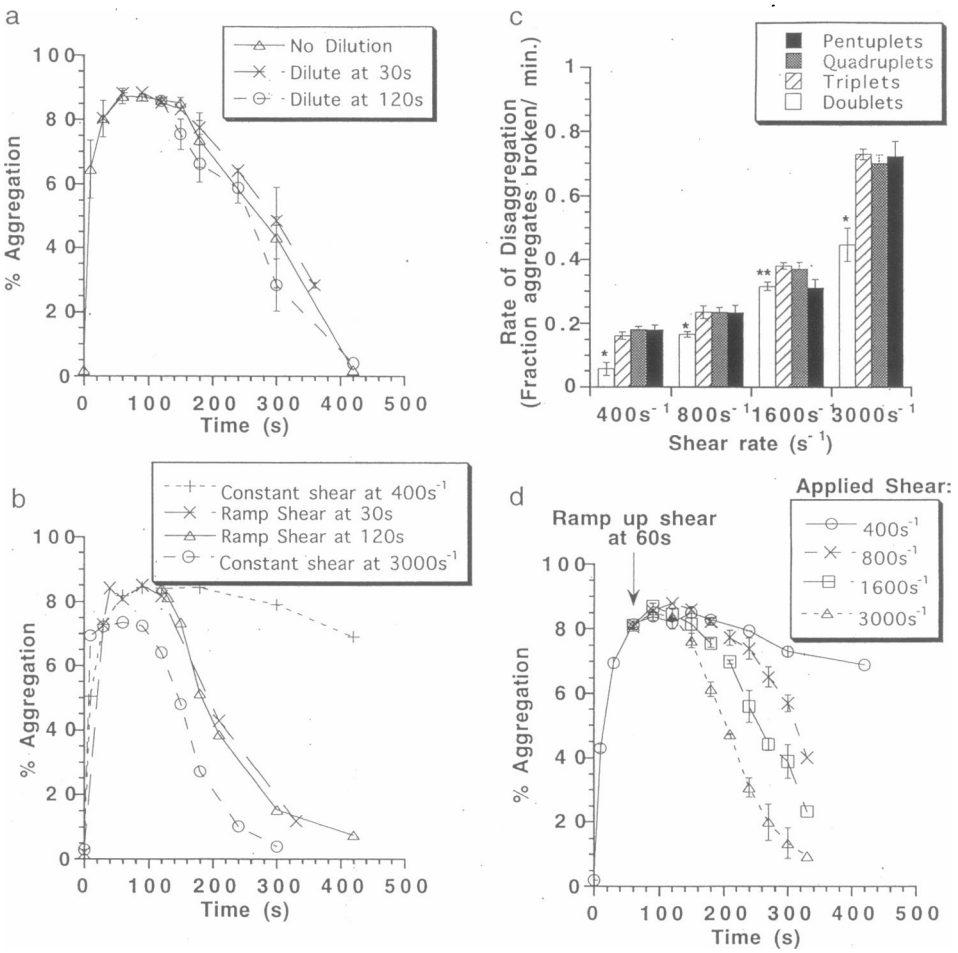

FIGURE 5 Kinetic studies of disaggregation. (*a*) Neutrophils at a concentration of 1×10^6 cells/ml were stimulated and sheared at $G = 1600\ s^{-1}$. The suspension was diluted 20 times in excess buffer containing 1 μM FMLP and 1.5 μM Ca^{2+} at either 30 s or 120 s. An undiluted control at $1600\ s^{-1}$ is also displayed. (*b*) Neutrophils at 1×10^6 cells/ml were stimulated and sheared at $G = 400\ s^{-1}$ for 30 s or 120 s before a ramp increase in the shear to $G = 3000\ s^{-1}$. In the controls, neutrophils were sheared at either $400\ s^{-1}$ or $3000\ s^{-1}$ throughout the time course. Data represent mean from three experiments. (*c*) Disaggregation rate quantified for each aggregate size (doublets to pentuplets), for 1×10^6 neutrophils/ml stimulated with 1 μM FMLP and sheared at $G = 400\ s^{-1}$ for 60 s before ramp increase in shear to $G = 800\ s^{-1}$, $1600\ s^{-1}$, or $3000\ s^{-1}$. Significance: *, $p < 0.05$ with respect to triplets, quadruplets, and pentuplets; **, $p < 0.05$ with respect to triplets and quadruplets. (*d*) Kinetics of disaggregation at the denoted shear rates for the ramp increase experiment described above, for $G = 400\ s^{-1}$, $800\ s^{-1}$, $1600\ s^{-1}$, $3000\ s^{-1}$. Error bars represent SEM from $N = 3$.

resistant to an increase in shear over the plateau phase. The disaggregation kinetics for both of the experiments in which shear was ramp increased at either 30 s or 120 s were identical to the controls in which cells were constantly sheared at $3000\ s^{-1}$. These results indicate that the processes contributing to the decrease in adhesion strength and disaggregation at the 120-s time point were independent of the time at which the shear force is applied.

The effect of aggregate size and shear rate on disaggregation

We explored the dependence of the rate of disaggregation on aggregate size and applied shear rate at the end of the plateau phase. In both the dilution and the ramp-shear protocols and for all of the shear rates tested, we observed a similar change in the aggregate size distribution, characterized by a marked increase in the number of singlets (data not shown). We concluded that disaggregation occurred as an "erosion process" in which single cells detach from larger cell aggregates, resulting in a large number of singlets and a gradual decrease in the larger aggregates over time. At all of the shear rates tested, the changes in the aggregate size distribution were not indicative of a "splitting process" in which large aggregates would be expected to break up into fragments of comparable sizes.

To characterize disaggregation as a function of particle size, we computed the rate of change of each aggregate species over a unit time. For example, the disaggregation rate of pentuplets at $1600\ s^{-1}$ was measured by the fraction of pentuplets that were broken up between 120 s and 240 s, divided by 2 min. This analysis was applied to the disaggregation kinetics for the ramp-shear experiments, in which stimulated neutrophils were sheared at $400\ s^{-1}$ for 60 s before a step increase in shear to $800\ s^{-1}$, $1600\ s^{-1}$, or $3000\ s^{-1}$ (Fig. 5, *c* and *d*). A comparison of the disaggregation rates of aggregates ranging from doublets to pentuplets shows that doublets disaggregated significantly more slowly (~60%) than larger aggregates (Fig. 5 *c*). There was no significant difference between the disaggregation rates of aggregates larger than doublets. We confirmed these results in the dilution experiments in which the rate of disaggregation of doublets was again ~60% slower than the disaggregation rate of larger aggregates (data not shown). Based on these measurements, the disaggregation rate of neutrophil aggregates after the plateau phase at ~120 s was mathe-

matically expressed as

$$b_{ij}C_j = \begin{cases} 0.6K_dC_j & j = 2, \quad i = 1 \\ K_dC_j & j > 2, \quad i = 1, \quad j - 1. \\ 0 & \text{for all other } i, j \end{cases} \quad (9)$$

The disaggregation rate coefficient (K_d, s^{-1}) is independent of aggregate size and is solely a function of the shear rate applied. The rate of disaggregation was observed to increase with the applied shear rate (Fig. 5 *d*). To quantify K_d, we modeled the disaggregation kinetics of the ramp increase in shear experiments. For these simulations, the adhesion efficiency over the disaggregation phase was set to zero. There was an approximately linear relationship between the shear rate applied and the disaggregation coefficients, as summarized in Table 1. Similar results were observed in the dilution experiments. There was a less than 10% difference in the disaggregation coefficient calculated from the two types of experiments.

Modeling aggregation kinetics at high cell concentrations

One objective of modeling aggregation was to predict the kinetics of aggregation and disaggregation over a wide range of cell concentrations and applied shear rates. Second, by evaluating model parameters that were independent of cell concentration, it is possible to distinguish between the effects of hydrodynamics and biological factors that modulate cell adhesiveness. With this in mind, we modeled the kinetics of neutrophil aggregation in the first 60 s after stimulation over a 10-fold range of cell concentrations from 5×10^5 to 5×10^6 neutrophils/ml. In these simulations, the time-dependent changes in adhesion efficiency as previously measured (Fig. 4 *b*) were applied, and the disaggregation rate was set to zero (Fig. 6). At the lower cell concentration of 5×10^5 cells/ml and at a shear rate of 400 s^{-1}, the model prediction agreed within 5% of the experimental data. At a higher concentration of 5×10^6 cells/ml, the collision frequency increased by 100-fold (Eq. 5), and therefore the model predicted that ~85% of the aggregates are recruited into sextuplets$^+$ (Fig. 6). Measurement by flow cytometry, however, revealed that only 35% of the aggregates were incorporated into sextuplets$^+$ (Fig. 6). This discrepancy indicated that the time-dependent decrease in adhesion efficiency applied in the simulation was not sufficient to predict the aggregation kinetics at the higher cell concentrations greater than ~10^6 cells/ml.

We further examined the range of applicability of the existing model over a 10-fold range of shear rates at these cell concentrations. At a concentration of 5×10^5 cells/ml and over the entire range of shear rates from 400 s^{-1} to 3000 s^{-1}, the model was able to fit the observed kinetics of aggregation within an error of 10% (data not shown). At 1×10^6 cells/ml and at shear rates of ≥800 s^{-1}, the model

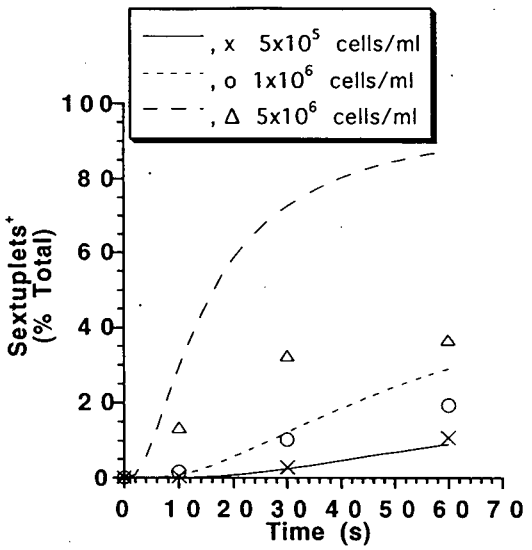

FIGURE 6 A model of the early kinetics of aggregation. Neutrophils at three different concentrations (5×10^5, 1×10^6, 5×10^6 cells/ml) were stimulated by 1 μM FMLP and sheared at 400 s^{-1}. The fraction of sextuplets$^+$ measured experimentally (denoted by *symbols*) are compared with simulation results (denoted by *lines*) from a model that only accounted for the time-dependent changes in adhesion efficiency.

prediction of sextuplets$^+$ overestimated the experimental measurement by more than 10% (data not shown). At a concentration of 5×10^6 neutrophils/ml, the model overpredicted experimental results over the entire range of shear rates.

It appeared that hydrodynamic shear severely limited the formation of large aggregates during the aggregation phase. For example, at a shear rate of 3000 s^{-1} and concentrations of 5×10^6 cells/ml, in spite of the large number of collisions we observed that less than 5% of the aggregates were quadruplets or larger. The effects of shear in limiting the formation of large aggregates appeared to be more pronounced at the higher cell concentrations, where the higher frequency of collisions supported their formation. To account for this effect we postulated that hydrodynamic shear affects aggregation kinetics, based on the geometry and size of the aggregates. Linear aggregates that are transiently formed immediately after cell collision (Fig. 3 *b*) are more susceptible to dissociation as compared to aggregates held together at multiple sites of attachment. We assumed that the elongated geometry of these transiently formed aggregates causes them to experience a larger torque. Furthermore, these aggregates should be held together by fewer bonds, because they are formed at single sites of attachment. This is supported by observations of aggregate geometry during the aggregation phase. At 30 s after stimulation, ~45% of the aggregates were held together at single points of attachment, whereas this percentage was reduced to ~15% at 180 s (Fig. 3). We hypothesize that linear aggregates of size j dissociate because of hydrodynamic shear

according to a power law expression:

$$b_{i,j}C_j = \frac{k j^m E}{i} C_j$$

$$j = 1, 2, 3 \ldots 15 \quad \text{and} \quad (10)$$

$$i = 1, 2, 3 \ldots 7.$$

The value of the breakage constant (k) was set at 4.8×10^{-3} s^{-1}, and the breakage exponent (m) was varied to fit the aggregation kinetics at each shear rate (Table 2). The dissociation term is proportional to the adhesion efficiency (E), because we expect that the fraction of aggregates of size j that have a linear geometry will be proportional to the rate at which they are formed. Because adhesion efficiency decreased rapidly after stimulation, the disaggregation term in Eq. 10 also decreases with time. Shear appeared to attenuate the rate of breakage in a nonlinear fashion, as indicated by the magnitude of the breakage exponent (m), which increased sharply with shear rate (Table 2).

Simulation of the entire kinetics of cell aggregation and disaggregation

The final objective was to model the time course of chemotactically stimulated neutrophil aggregation and disaggregation while taking into account the biological and biophysical features, including 1) the adhesion efficiency, which varied over time; 2) the break-up of transient aggregates over the aggregation phase; and 3) the disaggregation process in terms of aggregate size and shear rate. This model, based on experimentally derived adhesion and disaggregation parameters (listed in Tables 1 and 2), enabled us to simulate neutrophil aggregation kinetics. The simulation at 1×10^6 cells/ml and a shear rate of 800 s^{-1} yielded <10% difference between the experimentally measured aggregate size distribution and the model predictions (Fig. 7, *a* and *b*). At 5×10^6 cells/ml we observed that more than twice the number of sextuplets$^+$ were formed (Fig. 7, *c* and *d*). The experimental data agreed within 10% with the simulation predictions. The model parameters applied at all shear rates (listed in Tables 1 and 2) were independent of the cell concentration. A wider comparison of the model's predictions with the experimental data was performed over a ~10-fold range of shear rates (400–3000 s^{-1}) and cell concentrations (5×10^5 to 5×10^6 cells/ml), by using these parameters and the updated model. The aggregate size distribution predicted by the model differed from the experimental data by less than 10% over the entire time course of neutrophil aggregation.

TABLE 2 Simulation of the breakup of transiently formed aggregates

Shear rate, G (s^{-1})	Breakage constant, k (s^{-1})	Breakage exponent, m (dimensionless)
400	4.8×10^{-3}	1.5
800	4.8×10^{-3}	1.8
1600	4.8×10^{-3}	2.5
3000	4.8×10^{-3}	4.5

Neutrophils from 5×10^5 to 5×10^6 cells/ml were stimulated with 1 μM FMLP and sheared. Aggregation kinetics for the various cell concentrations were fit by modeling the breakup of transiently formed aggregates, as described in Eq. 10.

DISCUSSION

In the present study we formulated a mathematical model to predict the reversible time course of homotypic neutrophil aggregation after chemotactic stimulation in a linear shear field. Precise shearing of cell suspensions was achieved in a cone-plate viscometer over a range of shear rates from 400 s^{-1} to 3000 s^{-1}. Fluorescence flow cytometric analysis of glutaraldehyde-fixed samples provided quantitation of the temporal changes in the distribution of aggregate sizes from singlets to particles comprising six or more cells. The entire time course of aggregate formation and disaggregation was predicted based on an appropriate choice of model parameters and the experimental characterization of their dependence on time and shear rate.

A balance between molecular bonding and hydrodynamic forces determines the kinetics of aggregation

In this analysis the entire population of neutrophils is assumed to be composed of equally sized rigid spheres. Collision between any two spheres in a linear shear field will result in a transient doublet, the geometry of which is assumed to be a prolate ellipsoid (rodlike aggregate) (Jeffery, 1922). When sheared in a cone-plate viscometer, the doublet tumbles with a period that is independent of its size, but is dependent on the aggregate geometry and the applied shear rate. The mean lifetime of the transient doublet has been solved as $5\pi/6G$ (Bartok and Mason, 1957). This ranges from ~1 to 6 ms for the shear rates applied in our experiments (G = 400-3000 s^{-1}). Over one complete rotational orbit, neutrophil doublets experience hydrodynamic normal and shear forces. These forces vary sinusoidally with the angle of orientation of the axis of revolution of the particle with respect to the direction of flow throughout each half-orbit (Tees et al., 1993). Essentially, the rotating doublet experiences compressive forces during half of the cycle of rotation, and we presume that selectin and integrin bond formation occurs during this membrane contact. In addition, twice in each orbit the neutrophil experiences maximum tensile forces, which may act to rupture the bonds in the contact region between individual cells. Aggregates detected after fixation and flow cytometric analysis were only those that formed a sufficient number of bonds to overcome the tensile forces over successive cycles of rotation.

The initial rapid phase of aggregation

Single neutrophils were most rapidly recruited into aggregates over the initial phase of aggregation, which lasted up

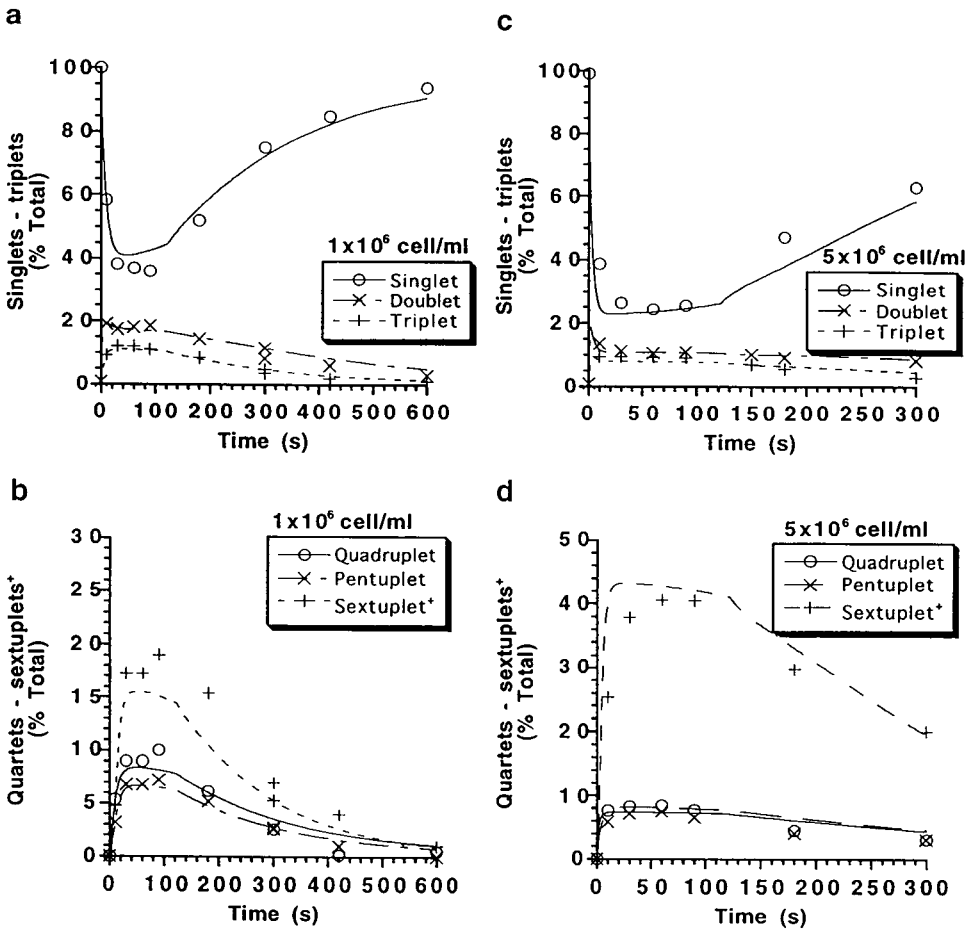

FIGURE 7 A model for the kinetics of aggregation and disaggregation. Experimental data (denoted by *symbols*) and model predictions (denoted by *lines*), for neutrophils stimulated by FMLP and subjected to shear at $G = 800\ s^{-1}$. Change in distribution of singlets-sextuplets$^+$ for neutrophils at a concentration of (*a,b*) 1×10^6 cells/ml, (*c,d*) 5×10^6 cells/ml. Experimental data represent mean for $N \geq 3$.

to ~30 s after formyl peptide stimulation. The rate of bond formation appears to far exceed the rate of bond breakage, as indicated by the high adhesion efficiency (E_0) used to model the early aggregation kinetics (Fig. 4 and Table 1). Efficiency decreased linearly with time after stimulation (Fig. 4 *b*), implying that the adhesiveness of the molecules supporting aggregation also decreased linearly. We had postulated in earlier studies that the rapid shedding of L-selectin was a key event mediating the decrease in efficiency (Simon et al., 1992). Within 60 s of FMLP stimulation ~⅓ of the L-selectin receptors were shed, whereas β_2-integrin expression was up-regulated by approximately twofold, independently of the applied shear rate (Taylor et al., 1996). Recent studies in our laboratory indicate that although the expression of integrins is up-regulated, its avidity decreases over the time course after stimulation. To measure the decrease in cell adhesiveness independently of the effect of L-selectin shedding, we treated neutrophils with a metalloprotease inhibitor, KD-IX-73-4. This peptide blocks L-selectin shedding after chemotactic stimulation, while leaving the adhesive function of β_2-integrin unaltered (Feehan et al., 1996). Using a protocol analogous to the experiments in Fig. 4, in which shear mixing was delayed after neutrophil stimulation, we found that the metalloprotease inhibitor partially rescued neutrophil adhesion efficiency. For example, at a shear rate of 1600 s^{-1}, adhesion efficiency at 90 s was increased from 0.05 in the untreated sample to 0.2 in the presence of KD-IX-73-4. Because adhesion efficiency in the absence of L-selectin shedding still decreased by ~50% from the initial levels just after stimulation ($E_0 = 0.39$), we conclude that besides the shedding of L-selectin, β_2-integrin avidity is also down-modulated over time.

The initial adhesion efficiency, E_0, was found to be at a maximum at shear rates of 400 s^{-1} and 800 s^{-1}, and it decreased at the higher shears of 1600 s^{-1} and 3000 s^{-1}. An increase in shear rate may affect bond formation and adhesion efficiency in two ways. Although an increase in shear rate produces a concomitant increase in cell deformation during collision and consequently the number of receptor-ligand pairs which may interact, it simultaneously reduces the intercellular contact duration during cell collision (Taylor et al., 1996). In the range of shear rate between 400 s^{-1} and 800 s^{-1}, in which the adhesion efficiency was found to be constant, the effects of increased cell deformation on bond formation presumably balance the effects of reduced intercellular contact duration. At shear rates greater than 800 s^{-1}, the diminished contact duration and increased hydrodynamic forces reduced the adhesion efficiency (Table 1).

The decrease in adhesion efficiency with time was modeled as an exponentially decreasing function based on the adhesion exponent (α), which increased by equal increments of 0.006 on doubling the shear rate (Table 1). This implies that upon doubling the shear rate, the efficiency decreases by a constant factor proportional to the function $e^{-0.006t}$. The relation is similar to the decrease in the average intercellular contact duration ($\sim 5\pi/6G$), which also decreases by a constant factor (½) on doubling the shear rate. Therefore, the adhesion exponent (α) at shear ≥ 400 s^{-1} appears to characterize the effect of intercellular contact duration on efficiency with time and shear.

Adhesion efficiency and cell concentration

A discrepancy was evident in the simulations of the aggregation kinetics at the low and high cell concentrations. Two-body collision theory predicts that cell collisions are 100 times more frequent for a neutrophil suspension sheared at an initial concentration of 5×10^6 cells/ml as compared to 5×10^5 cells/ml (Eq. 5). Despite this relation, the observed efficiency at the high cell density was significantly lower than that predicted by the theory (Fig. 6). We considered several explanations, both biological and physical, to account for the decreased efficiency. This effect was not due to the presence of subpopulations of neutrophils that were refractory to stimulation or deficient in the necessary adhesive counter-structure. We observed that ~95% of the neutrophils were recruited into aggregates under optimum conditions. Another possibility is that neutrophils secrete an anti-adhesive inhibitory factor that limits the formation of large aggregates. An increase in the cell concentration would presumably increase the amount of the inhibitory factor in the supernatant to a critical level, thereby reducing the extent of aggregation. To test this hypothesis, 1×10^7 neutrophils/ml were stimulated with 1 μM FMLP for 3 min and centrifuged, and the supernatant was used to stimulate another neutrophil suspension at 1×10^6 cells/ml. The adhesion efficiency at the lower cell concentration in the presence of the supernatant was not significantly different from that of a control population stimulated with fresh FMLP (data not shown). Therefore it was unlikely that inhibitory factors secreted by the neutrophils played a role in down-modulating adhesion efficiency.

The change in aggregate geometry over time provided some insight into the molecular and hydrodynamic processes that limited aggregate size and adhesion efficiency. Within the first few seconds of stimulation, aggregates of all sizes were observed to consist of cells held together predominantly at single sites of attachment. It has been reported that the hydrodynamic forces (F_{hydr}) experienced by a doublet are proportional to the square of the radius of the individual cell, b ($F_{hydr} \alpha \mu G b^2$) (Tha and Goldsmith, 1986). Based on this analysis, we expect that in the case of a linear quadruplet, the normal force acting on bonds between spheres 2 and 3 at the center of the quadruplet is about four times that of a doublet. To account for the transient break-up of aggregates, we included a power law expression to model the breakup of large aggregates (Eq. 10). Power law expressions such as this one have been used by others to study the splitting of flocculants and to analyze the breakage in dispersed phase systems (Valentas et al., 1966; Pandya and Spielman, 1983). We observed that an increase in shear severely limited the rate of formation of larger aggregates. This was quantitated by the breakage exponent (m), which increased sharply and nonlinearly with shear (Table 2).

The plateau phase of aggregate stability

Within ~1 min of stimulation, aggregate formation was essentially complete and aggregates remained stable over the "plateau phase." Regardless of the shear at which they were formed, aggregates were resistant to breakup at shear rates up to 3000 s^{-1}, corresponding to stresses of ~20 dynes/cm^2. Even though the number and distribution of aggregates remained essentially constant over the plateau, dynamic changes have been demonstrated in aggregate morphology (Hoffstein et al., 1982), geometry (Fig. 3), and β_2-integrin topography (Hughes et al., 1992). During aggregate formation, linear aggregates minimized their surface area and assumed more spherical geometries, such that adjoining cells were connected at multiple sites of contact. This should serve to stabilize spherical or clumped aggregates and prolong their lifetime in the plateau phase. We hypothesize that after the first minute of stimulation, β_2-integrins do not function to recruit more cells in aggregates, but rather maintain formed aggregates in a stable configuration.

The disaggregation phase

Reversibility in cell aggregation is a prerequisite for cell motility and is a critical aspect of neutrophil function (Smith, 1992). A consistent observation is that disaggregation ensued at ~120 s, independently of the applied shear rate, cell concentration, or aggregate size distribution. The mechanism of breakup of neutrophils from larger aggregates apparently occurred by an "erosion process" that resulted predominantly in the release of singlets. This is supported by the observation of a dramatic increase in the number of single neutrophils over the disaggregation phase.

A distinct and universal change in cell morphology that coincides with disaggregation is that cells adopt a bipolar shape by the 3-min time point (Fig. 3 *c*). This was accompanied by a reduction in the area of cell-cell contact by approximately threefold compared to the aggregation phase. In all cases, the point of cell-cell attachment was away from the lamellipod region, which is enriched in cytoskeletal contractile proteins, including F-actin (Wang, 1985). The topography of the β_2-integrin also changes with time after chemotactic stimulus. Previously we have shown that after FMLP stimulation, latex beads bound to the β_2-integrin in a

random pattern on the neutrophil surface (Hughes et al., 1992). With incremental stimulation, the beads diffused to the rear of the bipolar cells away from the lamellipodia. Taken together, these data support a mechanism of disaggregation that involves at least three processes: 1) Integrin adhesivity reaches a peak after stimulation and decreases to a low level within minutes, resulting in a rate of bond breakage exceeding that of formation. 2) Simultaneously, integrin receptors diffuse and concentrate to a smaller area of membrane contact corresponding to the rear of the cell. Over the time course of stimulation this sequence may serve to decrease the total neutrophil surface area available for adhesion and increase the stress on intercellular bonds. 3) Eventually the number and strength of bonds are exceeded by the hydrodynamic forces, and disaggregation occurs.

The rate of disaggregation was found to increase linearly with the applied shear rate and was directly correlated with the increase in the hydrodynamic tensile forces ($F_{hydr}\alpha\mu Gb^2$) (Tha and Goldsmith, 1986). Hydrodynamic shear forces also act linearly with shear rate ($F_{shear}\alpha\mu Gb^2$). Cell surface receptors are free to orient themselves toward the surface, and it is possible that shear forces at the contact area may be turned into stresses on the bonds that are tensile. The disaggregation rate was found to be equivalent for aggregates larger than doublets. This could be due to the fact that before breakup, most aggregates have adopted a spherical geometry and therefore a weaker dependence on particle radius as compared to linear aggregates. Interestingly, the rate of disaggregation of doublets was ~60% lower than that of larger aggregates. The reason for this difference is not evident from the current data. However, if all cells contain the same number of activated β_2-integrin molecules, then doublets may adhere over portions of the cell surface that have a higher density of integrins, thereby making them more resistant to the hydrodynamic tensile forces.

In this report we present a methodology to measure and analyze the aggregation kinetics of neutrophils. Homotypic aggregation is a complex process, because receptor-dependent cell signaling leads within minutes to the synchronous adhesion and subsequent disaggregation of millions of cells. The combination of cone-plate viscometry, flow cytometry, and mathematical analysis provides a means of delineating between the roles of hydrodynamic shear and receptor avidity in modulating cell adhesion.

We would like to thank Dr. Alan R. Burns for helping to acquire the light microscopy images, Dr. Evan Evans for his intellectual input, and Dr. Kei Kishimoto for providing reagents.

This work was supported by National Institutes of Health grants AI23521, 5P50NS23327, AI31652, and HL42550, and a Whitaker Foundation grant awarded to SIS.

REFERENCES

Alon, R., D. A. Hammer, and T. A. Springer. 1995. Lifetime of the P-selectin-carbohydrate bond and its response to tensile force in hydrodynamic flow. *Nature.* 374:539–542.

Bargatze, R. F., S. Kurk, E. C. Butcher, and M. A. Jutila. 1994. Neutrophils roll on adherent neutrophils bound to cytokine-induced endothelial cells via L-selectin on the rolling cells. *J. Exp. Med.* 180:1785–1792.

Bartok, W., and S. G. Mason. 1957. Particle motions in sheared suspensions. V. Rigid rods and collision doublets of spheres. *J. Colloid Sci.* 12:243–262.

Bennett, T. A., C. M. Schammel, E. B. Lynam, D. A. Guyer, A. Mellors, B. Edwards, S. Rogelj, and L. A. Sklar. 1995. Evidence for a third component in neutrophil aggregation: potential roles of O-linked glycoproteins as L-selectin counter-structures. *J. Leukoc. Biol.* 58:510–518.

Butcher, E. C. 1991. Leukocyte-endothelial cell recognition: three (or more) steps to specificity and diversity. *Cell.* 67:1033–1036.

Chandrasekhar, S. 1943. Stochastic problems in physics and astronomy. *Rev. Mod. Phys.* 15:2–89.

Feehan, C., K. Darlak, J. Kahn, B. Walcheck, and T. K. Kishimoto. 1996. Shedding of the lymphocyte L-selectin adhesion molecule is inhibited by a hydroxamic acid-based protease inhibitor. *J. Biol. Chem.* 271: 7019–7024.

Finger, E. B., K. Puri, R. Alon, M. B. Lawrence, U. H. von Andrian, and T. A. Springer. 1996. Adhesion through L-selectin requires a threshold hydrodynamic shear. *Nature.* 379:266–269.

Hoffstein, S. T., R. S. Friedman, and G. Weissmann. 1982. Degranulation, membrane addition, and shape change during chemotactic factor-induced aggregation of human neutrophils. *J. Cell Biol.* 95:234–241.

Huang, P. Y., and J. D. Hellums. 1993. Aggregation and disaggregation kinetics of human blood platelets. Part I. Development and validation of a population balance method. *Biophys. J.* 65:334–343.

Hughes, B. J., J. C. Hollers, E. Crockett-Torabi, and C. W. Smith. 1992. Recruitment of CD11b/CD18 to the neutrophil surface and adherence-dependent cell locomotion. *J. Clin. Invest.* 90:1687–1696.

Jeffery, G. B. 1922. On the motion of ellipsoidal particles immersed in a viscous fluid. *Proc. R. Soc. Lond.* A102:162–179.

Jones, D. A., O. Abbassi, L. V. McIntire, R. P. McEver, and C. W. Smith. 1993. P-selectin mediates neutrophil rolling on histamine-stimulated endothelial cells. *Biophys. J.* 65:1560–1569.

Lawrence, M. B., and T. A. Springer. 1991. Leukocytes roll on a selectin at physiologic flow rates: distinction from and prerequisite for adhesion through integrins. *Cell.* 65:859–873.

Lollo, B. A., K. W. H. Chan, E. M. Hanson, V. T. Moy, and A. A. Brian. 1993. Direct evidence for two affinity states for lymphocyte function-associated antigen 1 on activated T cells. *J. Biol. Chem.* 268:1–8.

Pandya, J. D., and L. A. Spielman. 1983. Floc breakage in agitated suspensions: effect of agitation rate. *Chem. Eng. Sci.* 38:1983–1992.

Rochon, Y. P., and M. M. Frojmovic. 1991. Dynamics of human neutrophil aggregation evaluated by flow cytometry. *J. Leukoc. Biol.* 50:434–443.

Rochon, Y. P., and M. M. Frojmovic. 1993. Regulation of human neutrophil aggregation: comparable latent times, activator sensitivities, and exponential decay in aggregability for FMLP, platelet-activating factor, and leukotriene B_4. *Blood.* 82:3460–3468.

Shampine, L. F., H. A. Watts, and S. M. Davenport. 1976. Solving non-stiff ordinary differential equations the state of the art. *SIAM Rev.* 18: 376–441.

Simon, S. I., A. R. Burns, A. D. Taylor, P. K. Gopalan, E. B. Lynam, L. A. Sklar, and C. W. Smith. 1995. L-selectin (CD62L) cross-linking signals neutrophil adhesive functions via the Mac-1 (CD11b/CD18) β_2-integrin. *J. Immunol.* 155:1502–1514.

Simon, S. I., J. D. Chambers, E. Butcher, and L. A. Sklar. 1992. Neutrophil aggregation is β_2-integrin- and L-selectin-dependent in blood and isolated cells. *J. Immunol.* 149:2765–2771.

Simon, S. I., J. D. Chambers, and L. A. Sklar. 1990. Flow cytometric analysis and modeling of cell-cell adhesive interactions: the neutrophil as a model. *J. Cell Biol.* 111:2747–2756.

Simon, S. I., Y. P. Rochon, E. B. Lynam, C. W. Smith, D. C. Anderson, and L. A. Sklar. 1993. β_2-Integrin and L-selectin are obligatory receptors in neutrophil aggregation. *Blood.* 82:1097–1106.

Simon, S. I., and G. W. Schmid-Schönbein. 1988. Biophysical aspects of microsphere engulfment by human neutrophils. *Biophys. J.* 53:163–173.

Sklar, L. A., G. M. Omann, and R. G. Painter. 1985. Relationship of actin polymerization and depolymerization to light scattering in human

neutrophils: dependence on receptor occupancy and intracellular Ca^{++}. *J. Cell Biol.* 101:1161–1166.

Smith, C. W. 1992. Transendothelial migration. *In* Adhesion: Its Role in Inflammatory Disease. J. M. Harlan and D. Y. Liu, editors. W. H. Freeman and Company, New York. 85–115.

Smoluchowski, M. V. 1917. Versuch einer mathematischen theorie der koagulationskinetik kolloider losungen. *Z. Phys. Chem.* 92:129–168.

Springer, T. A. 1995. Traffic signals on endothelium for lymphocyte recirculation and leukocyte emigration. *Annu. Rev. Physiol.* 57: 827–872.

Taylor, A. D., S. Neelamegham, J. D. Hellums, C. W. Smith, and S. I. Simon. 1996. Molecular dynamics of the transition from L-selectin to β_2-integrin dependent neutrophil adhesion under defined hydrodynamic shear. *Biophy. J.* 71:3488–3500.

Tees, D. F. J., O. Coenen, and H. L. Goldsmith. 1993. Interaction forces between red cells agglutinated by antibody. IV. Time and force dependence of break-up. *Biophys. J.* 65:1318–1334.

Tha, S. P., and H. L. Goldsmith. 1986. Interaction forces between red cells agglutinated by antibody. I. Theoretical. *Biophys. J.* 50:1109–1116.

Valentas, K. J., O. Bilous, and N. R. Amundson. 1966. Analysis of breakage in dispersed phase systems. *Ind. Eng. Chem. Fund.* 5:271–279.

von Andrian, U. H., J. D. Chambers, L. M. McEvoy, R. F. Bargatze, K.-E. Arfors, and E. C. Butcher. 1991. Two step model of leukocyte-endothelial cell interaction in inflammation: distinct roles for LECAM-1 and the leukocyte beta-2 integrins in vivo. *Proc. Natl. Acad. Sci. USA.* 88:7538–7542.

Walcheck, B., K. L. Moore, R. P. McEver, and T. K. Kishimoto. 1996. Neutrophil-neutrophil interactions under hydrodynamic shear stress involve L-selectin and PSGL-1. A mechanism that amplifies initial leukocyte accumulation on P-selectin in vitro. *J. Clin. Invest.* 98:1081–1087.

Wang, Y. L. 1985. Exchange of actin subunits at the leading edge of living fibroblasts: possible role of treadmilling. *J. Cell Biol.* 101:597–602.

Wei, J., W. Lee, and F. J. Krambeck. 1977. Catalyst attrition and deactivation in fluid catalytic cracking system. *Chem. Eng. Sci.* 32:1211–1218.